

# First Synthesis and Structural Determination of a Monomeric, Unsolvated Lithium Amide, LiNH<sub>2</sub>

Douglas B. Grotjahn,<sup>\*,†</sup> P. M. Sheridan,<sup>‡</sup> I. Al Jihad,<sup>‡</sup> and L. M. Ziurys<sup>\*,‡</sup>

Contribution from the Department of Chemistry, San Diego State University, 5500 Campanile Drive, San Diego, California 92182-1030, and Departments of Chemistry and Astronomy and Steward Observatory, 933 North Cherry Avenue, University of Arizona, Tucson, Arizona 85721

Received September 18, 2000

**Abstract:** Alkali metal amides typically aggregate in solution and the solid phase, and even in the gas phase. In addition, even in the few known monomeric structures, the coordination number of the alkali metal is raised by binding of Lewis-basic solvent molecules, with concomitant changes in structure. In contrast, the simplest lithium amide LiNH<sub>2</sub> has never been made in a monomeric form, even though its structure has been theoretically predicted several times. Here, the first experimental structural data for a monomeric, unsolvated lithium amide are determined using a combination of gas-phase synthesis and millimeter/submillimeter-wave spectroscopy. All data point to a planar structure for LiNH<sub>2</sub>. The r<sub>0</sub> structure of LiNH<sub>2</sub> has a Li–N distance of 1.736(3) Å, an N–H distance of 1.022(3) Å, and a H–N–H angle of 106.9(1)°. These results are compared with theoretical predictions for LiNH<sub>2</sub>, and experimental data for oligomeric, solid-phase samples, which could not resolve the question of whether LiNH<sub>2</sub> is planar or not. In addition, comparisons are made with revised gas-phase and solid-phase data and calculated structures of NaNH<sub>2</sub>.

## Introduction

Alkali metal amides have played a prominent role in the development of chemistry as a science.<sup>1–4</sup> Sodium and potassium amide were first reported at the beginning of the 19th century by Gay-Lussac and Thénard and independently by Davy, who used the new substances to reach conclusions about the constitutions of sodium, potassium, and ammonia.<sup>1</sup> Lithium amide was first made at the end of the last century.<sup>5</sup> The three-dimensional structures of solid alkali metal amides were first examined by IR spectroscopy<sup>6</sup> and NMR spectroscopy in the 1950s.<sup>7</sup> In addition, X-ray crystallography<sup>8–10</sup> showed the distorted cubic close-packing of amide anions and the presence of alkali cations in tetrahedral holes between the anions. Thus, each ion is associated with several ions of the opposite charge. Later refinement of the crystal structure of LiNH<sub>2</sub><sup>11</sup> suggested that the variation in orientation of NH<sub>2</sub> groups in the crystal is dictated by the packing of the ions in the unit cell, making it impossible to form conclusions about the structure of the hypothetical monomer. Continuing this theme, derivatives of lithium amide with substituents on the nitrogen show a beautiful variety of aggregated structures both in the solid state and in

solution,<sup>12–18</sup> with hexagonal prisms, ladders, and other evocative names used to describe the architectures seen. In fact, only a handful of crystallographically characterized monomeric lithium amides are known;<sup>12,14–17</sup> three examples are shown in Scheme 1.<sup>19–21</sup> These unusual structures, all featuring solvent molecule(s) such as THF or amines coordinated to lithium, are the result of employing sterically demanding and/or electronically stabilizing substituents at the anionic nitrogen of the amide ligand. In contrast, neither monomeric lithium nor sodium amide is known, although the lithium compound has been proposed (without direct evidence) to have been generated in an argon matrix by irradiating a lithium–ammonia adduct.<sup>22</sup> Computational studies of lithium amide as a prototypical alkali metal amide have focused on dimers,<sup>23,24</sup> trimers,<sup>24</sup> tetramers,<sup>25</sup> or hexamers.<sup>26</sup>

Lithium and sodium amide became important reagents in organic synthesis, rather than laboratory curiosities, because they were found to deprotonate ketones, aldehydes, and structurally

(12) Gregory, K.; Schleyer, P. v. R.; Snaith, R. *Adv. Inorg. Chem.* **1991**, 37, 47–142.

(13) Collum, D. B. *Acc. Chem. Res.* **1993**, 26, 227–234.

(14) Pauer, F.; Power, P. P. Structures of Lithium Salts of Heteroatom Compounds. In *Lithium Chemistry: A Theoretical and Experimental Overview*; Sapse, A.-M., Schleyer, P. v. R., Eds.; Wiley: New York, 1995; pp 295–392.

(15) Beswick, M. A.; Wright, D. S. Alkali Metals. In *Comprehensive Organometallic Chemistry II*; Abel, E. W., Stone, F. G. A., Wilkinson, G., Eds.; Pergamon: New York, 1995; Vol. 1.

(16) Mulvey, R. E. *Chem. Soc. Rev.* **1991**, 20, 167–209.

(17) Mulvey, R. E. *Chem. Soc. Rev.* **1998**, 27, 339–346.

(18) Clegg, W.; Liddle, S. T.; Mulvey, R. E.; Robertson, A. *J. Chem. Soc., Chem. Commun.* **1999**, 511–512.

(19) Fjeldberg, T.; Hitchcock, P. B.; Lappert, M. F.; Thorne, A. J. *J. Chem. Soc., Chem. Commun.* **1984**, 822–824.

(20) Chen, H.; Bartlett, R. A.; Dias, H. V. R.; Olmstead, M. M.; Power, P. P. *J. Am. Chem. Soc.* **1989**, 111, 4338–4345.

(21) Andrews, P. C.; Duggan, P. J.; Fallon, G. D.; McCarthy, T. D.; Peatt, A. C. *J. Chem. Soc., Dalton Trans.* **2000**, 1937–1940.

(22) Meier, P. F.; Hauge, R. H.; Margrave, J. L. *J. Am. Chem. Soc.* **1978**, 100, 2108–2112.

<sup>†</sup> San Diego State University.

<sup>‡</sup> University of Arizona.

(1) Bergstrom, F. W.; Fernelius, W. C. *Chem. Rev.* **1933**, 12, 43–179.

(2) Juza, R. *Angew. Chem., Int. Ed. Engl.* **1964**, 3, 471–481.

(3) Lappert, M. F.; Power, P. P.; Sanger, A. R.; Srivastava, R. C. *Metal and Metalloid Amides*; Ellis Horwood: Chichester, 1980.

(4) Bram, G.; Bataille, X. C. *R. Acad. Sci. Paris, Ser. IIB* **1997**, 324, 653–657.

(5) Titherly, A. W. *J. Chem. Soc.* **1894**, 65, 504–522.

(6) Mason, S. F. *J. Phys. Chem.* **1957**, 61, 384.

(7) Freeman, R.; Richards, R. E. *Trans. Faraday Soc.* **1956**, 52, 802–807.

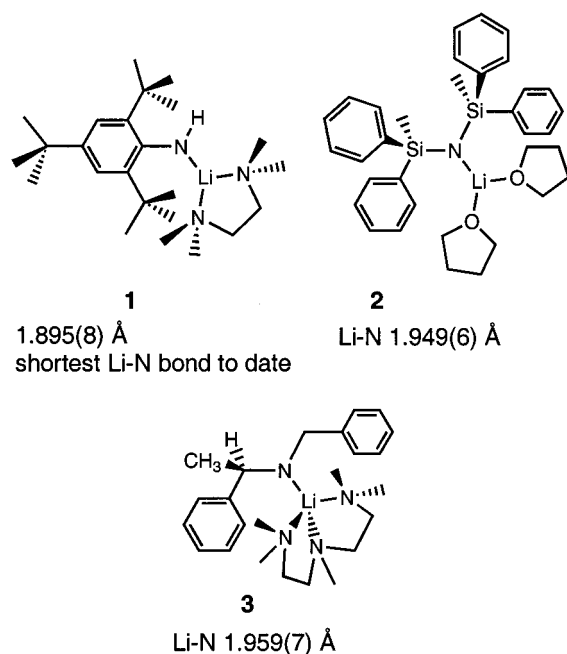
(8) Juza, R.; Opp, K. Z. *Anorg. Allg. Chem.* **1951**, 313–324.

(9) Juza, R.; Weber, H. H.; Opp, K. Z. *Anorg. Allg. Chem.* **1956**, 284, 72–82.

(10) Zalkin, A.; Templeton, D. H. *J. Phys. Chem.* **1956**, 60, 821–823.

(11) Jacobs, H.; Juza, R. Z. *Anorg. Allg. Chem.* **1972**, 391, 271–279.

## Scheme 1



related organic molecules.<sup>27–32</sup> Sodium amide has been described as leading to the birth of strong-base chemistry.<sup>4</sup> Depending on the application, either lithium amide<sup>33,34</sup> or sodium amide<sup>35,36</sup> has been found to be superior.

The use of large groups on the amide nitrogen frequently results in regioselective and stereoselective deprotonation in reactions under kinetic control.<sup>28</sup> The enolates so produced are versatile species in organic synthesis, for example, as precursors to regio- and stereodefined enolates of silicon, boron, or other elements, which in turn can control subsequent carbon–carbon bond-forming reactions. Recent developments in alkali metal amide chemistry have focused on the use of chiral amides for processes such as deprotonation<sup>37–39</sup> or reduction.<sup>40</sup> If a synthetic chemist wishes to reverse a 10:1 ratio of products to 1:10, at  $-78\text{ }^{\circ}\text{C}$ , a common temperature for use of alkali metal amides, a change in  $\Delta G^{\ddagger}$  for two alternate transition states of only 1.8

kcal mol<sup>-1</sup> is required. Clearly, a subtle change in structure (e.g., bond lengths and angles) could lead to dramatic change in the free energy changes involved, and hence a sharp reversal of selectivity. Theoretical calculations attempting to model subtle structural features will rely on comparisons of calculated structures for simpler molecules with precise experimental data such as those provided in this paper.

Regardless of the specific application, understanding the structure of the alkali amides is crucial to controlling selectivity. Elegant and difficult studies by the groups of Collum,<sup>13</sup> Hilmersson and Davidsson,<sup>41,42</sup> Klumpp,<sup>43</sup> and others are elucidating the solution structures of lithium amides. However, because solution structure studies do not give information about bond lengths and angles, only on atom connectivity and equilibria between species, other techniques are needed to compare theoretical and actual geometries. In this paper we report the first synthesis of an unsolvated, monomeric lithium amide, LiNH<sub>2</sub>. This is possible only in the gas phase, where millimeter/submillimeter spectroscopy was used to precisely determine bond lengths and angles. Precise experimental data on the bond lengths and angles of gas-phase monomers will allow refinement of theoretical calculations. The data presented here are the first available for LiNH<sub>2</sub>, a key model compound for larger amides used in synthesis.

## Experimental Section

The pure rotational spectra of LiNH<sub>2</sub> and LiND<sub>2</sub> were measured using a millimeter/submillimeter-wave absorption spectrometer, parts of which are described elsewhere in detail.<sup>44</sup> Briefly, the source of tunable millimeter-wave radiation is a phase-locked Gunn oscillator used in conjunction with a Schottky diode multiplier. Several Gunn oscillators and multipliers are necessary to cover the frequency range of 100–550 GHz. The radiation is launched from a scalar feedhorn with a Gaussian beam shape and is passed through a wire polarizing grid. Using two offset ellipsoidal mirrors, the radiation is quasi-optimally propagated through the reaction chamber, which is a double-pass system and is water-cooled. A roots-type blower pumping system continuously evacuates the cell. The molecules are created in this chamber which contains a Broida-type oven. The oven is used to vaporize metals by resistive heating. A rooftop reflector at the back of the cell changes the polarization of the radiation by 90° and reflects it back through the cell and mirror optics and into a liquid helium cooled InSb bolometer detector. The radiation source is frequency modulated at 25 kHz and data are recorded as second derivative spectra using a lock-in amplifier. The path length through the spectrometer system is additionally modulated using a movable rooftop reflector, located at the beam waist between the two mirrors, to improve the baseline.

LiNH<sub>2</sub> was synthesized in the gas phase by the reaction of lithium and ammonia, with argon serving as the carrier gas. The lithium vapor was created by heating solid lithium in the Broida-type oven.<sup>44</sup> The lithium vapor was entrained in a 1:1 mixture of ammonia and argon, added over the top of the oven. About 10 mTorr of each gas was used. The molecule was synthesized continuously in the reaction cell for as long as lithium vapor was present (1 to 2 h). Molecule lifetimes are estimated to be less than 1 s. For LiND<sub>2</sub>, the same procedure was

(23) Kaufmann, E.; Clark, T.; Schleyer, P. v. R. *J. Am. Chem. Soc.* **1984**, *106*, 1856–1858.

(24) Sapse, A.-M.; Kaufmann, E.; Schleyer, P. v. R.; Gleiter, R. *Inorg. Chem.* **1984**, *23*, 1569–1574.

(25) Sapse, A.-M.; Raghavachari, K.; Schleyer, P. v. R.; Kaufmann, E. *J. Am. Chem. Soc.* **1985**, *107*, 6483–6486.

(26) Raghavachari, K.; Sapse, A.-M.; Jain, D. C. *Inorg. Chem.* **1987**, *26*, 2585–2588.

(27) Fieser, L.; Fieser, M. *Reagents for Organic Synthesis*; Wiley: New York, 1967; Vol. 1.

(28) Gray, M.; Tinkl, M.; Snieckus, V. Lithium. In *Comprehensive Organometallic Chemistry II*; Abel, E. W., Stone, F. G. A., Wilkinson, G., Eds.; Pergamon: New York, 1995; Vol. 11.

(29) Erden, I. Lithium Amide. In *Encyclopedia of Reagents for Organic Synthesis*; Paquette, L. A., Ed.; Wiley: New York, 1995; Vol. 5, pp 3031–3034.

(30) Erden, I. Lithium Amide. In *Handbook of Reagents for Organic Synthesis: Acidic and Basic Reagents*; Reich, H. J., Rigby, J. H., Eds.; Wiley: Chichester, 1999; Vol. 3, pp 204–206.

(31) Belletire, J. L.; Rauh, R. J. Sodium Amide. In *Encyclopedia of Reagents for Organic Synthesis: Acidic and Basic Reagents*; Reich, H. J., Rigby, J. H., Eds.; Wiley: Chichester, 1999; Vol. 3, pp 329–332.

(32) Hauser, C. R.; Puterbaugh, W. H. *J. Am. Chem. Soc.* **1953**, *75*, 1068–1072.

(33) Herbrandson, H. F.; Mooney, D. S. *J. Am. Chem. Soc.* **1957**, *79*, 5809–5814.

(34) Harris, S. R.; Levine, R. *J. Am. Chem. Soc.* **1948**, *70*, 3360–3361.

(35) Hamell, M.; Levine, R. *J. Org. Chem.* **1950**, *15*, 162–168.

(37) Koga, K. *Pure Appl. Chem.* **1994**, *66*, 1487–1492.

(38) Hodgson, D. M.; Gibbs, A. R.; Drew, M. G. B. *J. Chem. Soc., Perkin Trans. 1* **1999**, 3579–3590.

(39) Vedejs, E.; Lee, N. *J. Am. Chem. Soc.* **1995**, *117*, 891–900.

(40) Takeda, K.; Ohnishi, Y.; Koizumi, T. *Org. Lett.* **1999**, *1*, 237–239.

(41) Hilmersson, G.; Arvidsson, P. I.; Davidsson, O.; Håkansson, M. *Organometallics* **1997**, *16*, 3352–3362.

(42) Arvidsson, P. I.; Ahlberg, P.; Hilmersson, G. *Chem. Eur. J.* **1999**, *5*, 1348–1354.

(43) van Vliet, G. L. J.; de Kanter, F. J. J.; Schakel, M.; Klumpp, G. W.; Spek, A. L.; Lutz, M. *Chem. Eur. J.* **1999**, *5*, 1091–1094.

(44) Ziurys, L. M.; Barclay, W. L., Jr.; Anderson, M. A.; Fletcher, D. A.; Lamb, J. W. *Rev. Sci. Instrum.* **1994**, *65*, 1517–1522.

followed, using ND<sub>3</sub> rather than NH<sub>3</sub>. Line intensities were typically weaker for the deuterated species.

Final transition frequency measurements were obtained from scans 5 MHz in frequency coverage. One scan in increasing frequency and one in decreasing frequency were typically averaged together. For weaker lines, particularly at lower frequencies, the number of scans was increased to eight or twelve. All line profiles were fit to Gaussian shapes to determine the center. Line widths ranged from 400 to 1400 kHz over 114–535 GHz.

## Results and Discussion

**Synthesis.** Theoretical calculations suggested that vaporizing monomeric LiNH<sub>2</sub> from the dimer,<sup>23,24</sup> trimer,<sup>24</sup> tetramer,<sup>25</sup> or hexamer<sup>26</sup> would be difficult if not impossible, a situation also encountered in simple alkylolithiums such as CH<sub>3</sub>Li.<sup>45</sup> Therefore, rather than attempting to vaporize the monomer from a solid-phase sample, we prepared LiNH<sub>2</sub> or LiND<sub>2</sub> directly in the gas phase by reaction of gaseous NH<sub>3</sub> or ND<sub>3</sub> and lithium vapor. A dc discharge was unnecessary, unlike in the previously reported synthesis of NaNH<sub>2</sub> from ammonia and sodium.<sup>46</sup> Details of the synthesis are found in the Experimental Section.

**Analysis of the Data.** Table 1 shows the observed transitions for both LiNH<sub>2</sub> and LiND<sub>2</sub>. Assuming both isotopomers are near prolate asymmetric top species with C<sub>2v</sub> symmetry and <sup>1</sup>A<sub>1</sub> ground electronic states, the quantum numbers which describe the rotational transitions of this molecule are *J*, *K<sub>a</sub>*, and *K<sub>c</sub>*. *J* represents the total angular momentum of the molecule, exclusive of nuclear spin. *K<sub>a</sub>* and *K<sub>c</sub>* are projections of *J* onto the symmetry axis of the molecule in the respective prolate and oblate symmetric top limits. In the case of an asymmetric top, *K<sub>a</sub>* and *K<sub>c</sub>* are no longer well defined and serve only as energy level labels.

As described below, all evidence suggests that the molecule is planar; hence, the dipole moment only lies along the *a*-axis and rotational transitions follow *a*-type selection rules ( $\Delta K_a = 0$ ,  $\Delta K_c = \pm 1$ ). Since  $\Delta K_a = 0$ , asymmetry components can be labeled by the *K<sub>a</sub>* quantum number. In a low *J* transition of a near prolate asymmetric top, the *K<sub>a</sub>* = 0 component appears approximately at the center between the two asymmetrically split *K<sub>a</sub>* = 1 components. Other *K<sub>a</sub>* components progress lower in frequency from the *K<sub>a</sub>* = 0 component with decreased splitting. However, as *J* increases, so does the asymmetry doubling. This results in the *K<sub>a</sub>* = 0 component shifting lower in frequency, often lower than higher *K<sub>a</sub>* components. This effect is also increased on deuteration, since the molecule becomes more asymmetric relative to the center of mass.

Identifying this asymmetric top pattern was not trivial for LiNH<sub>2</sub> or LiND<sub>2</sub> because of the relatively large rotational constants for these species. The initial search for LiNH<sub>2</sub> began by searching 150 GHz of frequency space, which is approximately 6*B* of the estimated rotational constant of 28–31 GHz, based on other alkaline-earth amide species.<sup>46</sup> *K<sub>a</sub>* components in adjacent transitions were identified by establishing harmonic relationships between lines fit with effective rotational constants in this range. Once several of these relationships were determined, preliminary assignment of the *K<sub>a</sub>* quantum number was made. This assignment was aided by the effect of nuclear spin statistics on the spectrum. A C<sub>2</sub> rotation of LiNH<sub>2</sub> results in the exchange of the two protons, which are fermions (*I* = 1/2). The total wave function, which describes the molecule, must be antisymmetric to this exchange. Thus, the ortho energy levels, which the odd *K<sub>a</sub>* components arise from, have a degeneracy of

**Table 1.** Observed Transition Frequencies of LiNH<sub>2</sub> and LiND<sub>2</sub> (X<sup>1</sup>A<sub>1</sub>)<sup>a</sup>

<i>J</i> '	<i>K<sub>a</sub></i> '	<i>K<sub>c</sub></i> '	<i>J</i> ''	<i>K<sub>a</sub></i> ''	<i>K<sub>c</sub></i> ''	LiNH <sub>2</sub>		LiND <sub>2</sub>	
						<i>ν</i> <sub>obs</sub>	<i>ν</i> <sub>obs</sub> - <i>ν</i> <sub>calc</sub>	<i>ν</i> <sub>obs</sub>	<i>ν</i> <sub>obs</sub> - <i>ν</i> <sub>calc</sub>
2	1	2	1	1	1	114201.204	-0.053		
2	0	2	1	0	1	116584.433	-0.032		
4	1	4	3	1	3	228354.543	-0.006		
4	3	1	3	3	0	232238.853	-0.172		
4	3	2	3	3	1	232238.853	0.007		
4	2	3	3	2	2	232738.999	0.038		
4	2	2	3	2	1	232847.806	-0.006		
4	0	4	3	0	3	233050.121	-0.037		
4	1	3	3	1	2	237718.425	0.003		
5	1	5	4	1	4	285398.338	-0.007		
5	4	2	4	4	1	289320.694	-0.028		
5	4	1	4	4	0	289320.694	-0.028		
5	2	4	4	2	3	290884.950	0.068		
5	2	3	4	2	2	291102.487	0.004		
5	0	5	4	0	4	291201.418	-0.020		
5	1	4	4	1	3	297097.236	0.020		
6	1	6	5	1	5	342412.422	-0.002	290701.606	-0.037
6	5	2	5	5	1	345621.312	-0.043	298974.311	0.041
6	5	1	5	5	0	345621.312	-0.043	298974.311	0.040
6	4	3	5	4	2	347158.453	0.018	299896.615	0.036
6	4	2	5	4	1	347158.453	0.016	299896.615	-0.075
6	3	4	5	3	3	348318.508	-0.089	300663.792	-0.083
6	3	3	5	3	2	348320.251	-0.023	300687.971	-0.031
6	2	5	5	2	4	349005.022	0.089	300672.097	-0.039
6	0	6	5	0	5	349278.714	-0.001	299548.872	-0.064
6	2	4	5	2	3	349385.480	0.005	302366.461	-0.041
6	1	5	5	1	4	356441.919	-0.071	310847.718	-0.051
7	1	7	6	1	6	399391.023	0.006	338952.389	-0.007
7	6	2	6	6	1			347504.282	0.023
7	6	1	6	6	0			347504.282	0.023
7	5	3	6	5	2			348809.359	0.037
7	5	2	6	5	1			348809.359	0.036
7	4	4	6	4	3	404981.773	0.052	349901.743	0.165
7	4	3	6	4	2	404981.773	0.044	349901.743	-0.204
7	3	5	6	3	4	406341.204	-0.015	350825.860	-0.006
7	3	4	6	3	3	406344.942	-0.050	350880.141	0.002
7	2	6	6	2	5	407094.058	0.106	350633.416	0.015
7	0	7	6	0	6	407267.422	-0.007	348713.754	0.011
7	2	5	6	2	4			353329.057	0.009
7	1	6	6	1	5	415745.804	0.011	362417.626	0.029
8	1	8	7	1	7	456328.442	-0.009	387116.838	0.047
8	6	3	7	6	2			397146.489	-0.046
8	6	2	7	6	1			397146.489	-0.046
8	5	4	7	5	3	460739.072	0.083	398647.068	0.019
8	5	3	7	5	2	460739.072	0.083	398647.068	0.014
8	4	5	7	4	4	462788.237	0.072		
8	4	4	7	4	3	462788.237	0.050		
8	3	6	7	3	5	464349.347	0.008	401005.742	0.002
8	3	5	7	3	4	464356.889	0.007	401114.225	0.003
8	2	7	7	2	6	465146.843	0.060	400525.148	0.027
8	0	8	7	0	7	465153.279	0.032	397547.572	0.057
8	2	6	7	2	5	466057.952	0.031	404533.928	0.037
8	1	7	7	1	6	475001.586	-0.009	413871.289	0.020
9	1	9	8	1	8	513219.097	-0.066		
9	6	4	8	6	3			446788.086	-0.037
9	6	3	8	6	2			446788.086	-0.037
9	5	5	8	5	4	518270.164	-0.057	448487.780	0.014
9	5	4	8	5	3	518270.164	-0.057	448487.780	<0.000
9	4	6	8	4	5	520575.366	0.016	449943.108	0.018
9	4	5	8	4	4	520575.366	-0.036	449945.473	-0.054
9	3	7	8	3	6	522340.545	-0.029	451202.148	0.112
9	3	6	8	3	5	522354.373	-0.024	451400.742	0.046
9	0	9	8	0	8	522922.236	0.061	446024.286	0.057
9	2	8	8	2	7	523158.217	-0.062	450337.485	0.039
9	2	7	8	2	6	524457.508	0.047	455994.215	0.039
9	1	8	8	1	7	534202.217	-0.054	465187.728	0.035
10	1	10	9	1	9			483154.371	-0.050
10	0	10	9	0	9			494131.122	-0.028
10	6	5	9	6	4			496428.850	0.046
10	6	4	9	6	3			496428.850	0.046
10	5	6	9	5	5			498331.756	-0.002
10	5	5	9	5	4			498331.756	-0.040
10	4	7	9	4	6			499981.986	-0.001
10	4	6	9	4	5			499987.235	-0.037
10	2	9	9	2	8			500060.590	-0.028
10	3	8	9	3	7			501411.809	-0.023
10	3	7	9	3	6			501751.791	0.017
10	2	8	9	2	7			507709.574	-0.035
10	1	9	9	1	8			516343.921	-0.076

<sup>a</sup> In MHz.

(45) Chinn, J. W., Jr.; Lagow, R. *Organometallics* **1984**, *3*, 75–77.

(46) Xin, J.; Brewster, M. A.; Ziurys, L. M. *Astrophys. J.* **2000**, *530*, 323–328.

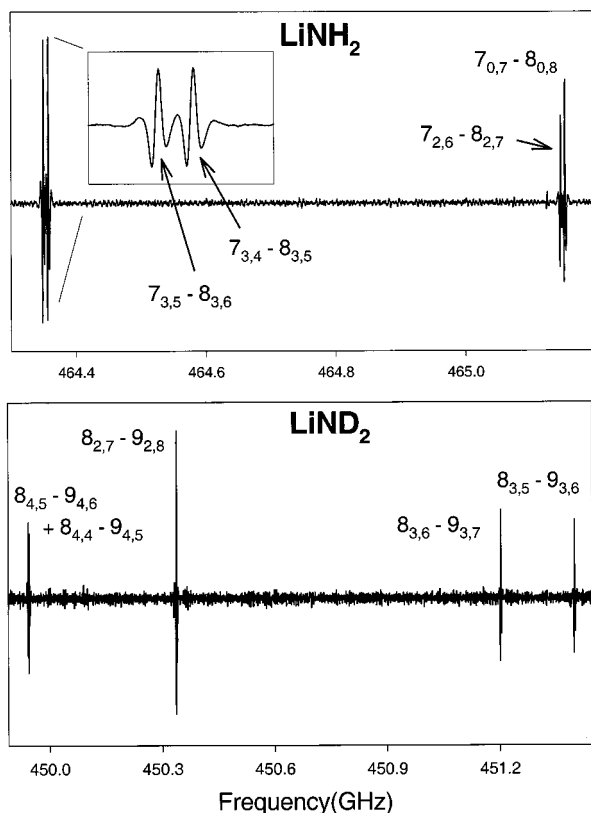


**Figure 1.** Spectra of a section of the  $J = 7-8$  transition of  $\text{LiNH}_2$  and part of the  $J = 8-9$  transition of  $\text{LiND}_2$ , near 465 and 451 GHz, respectively. The quantum number labeling is  $J_{K_a K_c}$ . In the  $\text{LiNH}_2$  spectrum, the  $K_a = 0$  and 3 components are present, as well as one component of the  $K_a = 2$  doublet. In the inset, the asymmetry splitting of the  $K_a = 3$  component near 464.4 GHz is shown, using an expanded scale. For  $\text{LiND}_2$ , one line for the  $K_a = 2$  doublet is visible but both components for  $K_a = 3$  and 4 are present. The effect of nuclear spin statistics, coupled with the Boltzmann factors, is evident in the data. For  $\text{LiNH}_2$ , the  $K_a$  odd lines are stronger than the  $K_a$  even ones; in the  $\text{LiND}_2$  spectrum, the opposite occurs. Both spectra are composites of 9 to 16, 100 MHz scans, each lasting approximately 1 min in duration.

$(I + 1)(2I + 1)$ , and the para or even  $K_a$  levels have a degeneracy of  $I(2I + 1)$ . This results in an approximate 3:1 intensity alteration of odd:even  $K_a$  components. Thus, the  $K_a = 1$  and 3 components were identified first. These preliminary assignments were then used to predict the frequencies of additional  $K_a$  components.

For  $\text{LiND}_2$ , nearly 160 GHz of frequency space was initially searched. The final fit of the rotational transitions for  $\text{LiND}_2$  was obtained by a procedure similar to that described for  $\text{LiNH}_2$ . However, for  $\text{LiND}_2$ , a  $C_2$  rotation results in the exchange of the two deuteriums, which are bosons ( $I = 1$ ), changing the intensity alteration by spin statistics to 2:1,  $K_a$  even: $K_a$  odd.

Although the spin statistics observed for both  $\text{LiNH}_2$  and  $\text{LiND}_2$  indicate that they are planar, a pyramidal structure, which undergoes a  $C_2$  rotation followed by molecular inversion, was also a possible geometric consideration. However, if the molecule were undergoing molecular inversion, an inversion spectrum with the opposite spin statistics of the ground state would be present. In the extensive search for these molecules, an inversion spectrum was not observed for either species. Further evidence for a planar geometry is provided by the observation of a small positive inertial defect with little change on deuterium substitution, which is usually a good indication of planarity.<sup>47,48</sup> For  $\text{LiNH}_2$ , the inertial defect  $\Delta = 0.115$  amu

**Table 2.** Rotational Constants for  $\text{LiNH}_2$  and  $\text{LiND}_2^a$

	$\text{LiNH}_2$	$\text{LiND}_2$
<i>A</i>	394567(49)	197378(3)
<i>B</i>	30321.626(20)	26795.004(23)
<i>C</i>	27978.631(19)	23428.339(20)
<i>D<sub>J</sub></i>	0.149451(69)	0.086981(53)
<i>D<sub>JK</sub></i>	12.9834(29)	7.9808(20)
<i>d<sub>1</sub></i>	-0.015485(74)	-0.017241(64)
<i>d<sub>2</sub></i>	-0.007830(42)	-0.01288(10)
<i>H<sub>KJ</sub></i>	-0.01807(26)	-0.003957(94)
<i>H<sub>JK</sub></i>	0.001003(19)	0.000706(19)
<i>h<sub>2</sub></i>		$1.64(74) \times 10^{-6}$
<i>h<sub>3</sub></i>	$4.3(2.7) \times 10^{-7}$	$7.4(1.5) \times 10^{-7}$
<i>L<sub>JK</sub></i>	$8.01(82) \times 10^{-6}$	$1.15(29) \times 10^{-6}$
<i>L<sub>KJK</sub></i>	$-3.981(69) \times 10^{-4}$	$-3.08(16) \times 10^{-5}$
<i>L<sub>JJK</sub></i>		$-2.02(81) \times 10^{-7}$
rms of fit	0.045	0.040

<sup>a</sup> In MHz; errors are  $3 - \sigma$  and apply to the last quoted decimal place.

$\text{\AA}^2$  and for  $\text{LiND}_2$ ,  $\Delta = 0.150$  amu  $\text{\AA}^2$ . These values are somewhat higher but comparable to those for  $\text{NaNH}_2$  (0.079 amu  $\text{\AA}^2$ )<sup>46</sup> and for formaldehyde (0.05767 amu  $\text{\AA}^2$ ),<sup>49</sup> both of which are planar. In contrast, for the nonplanar molecules  $\text{NH}_2\text{OH}$  and  $\text{NH}_2\text{Cl}$ , values of  $-2.600$  amu  $\text{\AA}^2$  or  $-1.032$   $\text{\AA}^2$ , respectively, have been found.<sup>50,51</sup>

Extra lines were observed in the spectra of  $\text{LiNH}_2$  and  $\text{LiND}_2$ , which may arise from the  $^6\text{Li}$  isotopomers. However, the ratio of  $^7\text{Li}$  and  $^6\text{Li}$  in the natural abundance samples used would be 12.3 to 1.<sup>52</sup> Any  $^6\text{Li}$  lines are therefore over an order of magnitude lower in intensity. While this reduced signal level may not pose a problem for strong  $K_a = 0$  and 1 components, the spectra could not be assigned without observing lines originating in the  $K_a = 4$  and 5 levels. Even in more abundant  $^7\text{LiNH}_2$  and  $^7\text{LiND}_2$ , the signals for these components were greatly reduced relative to the  $K_a = 0$  and 1 lines. Therefore it was not surprising that for the corresponding  $^6\text{Li}$  species these signals were not detectable.

Finally, quadrupole interactions due to both the  $^7\text{Li}$  ( $I = 3/2$ ) and the  $^{14}\text{N}$  ( $I = 1$ ) nuclei must be considered, in particular at low  $J$ . For  $\text{LiNH}_2$ , there was no evidence of quadrupole splitting in the  $J = 1 \rightarrow 2$  transition. The  $J = 0 \rightarrow 1$  transition, where such splitting is expected to be largest, was not recorded since it was below the attainable frequency range. Failure to observe quadrupole hyperfine interactions is not surprising. The dominant nucleus for this splitting should be  $^7\text{Li}$ , since it has a quadrupole moment a factor of 2 larger than that of  $^{14}\text{N}$ .<sup>52</sup> On the basis of data for  $\text{LiH}$ ,<sup>53</sup> the quadrupole coupling constant ( $eqQ$ ) in  $\text{LiNH}_2$  is estimated to be less than 350 kHz. Such a value would result in a splitting of  $<300$  kHz in the  $J = 2 \rightarrow 1$  transition, which would not be observable given the line widths of at least about 400 kHz at the  $J = 2 \rightarrow 1$  frequency.

For both species, the data were fit with a  $^1A_1$  Hamiltonian using the least-squares fitting program SPFIT. This Hamiltonian includes rotational constants and up to 4th order centrifugal distortion parameters. For  $\text{LiNH}_2$ , 57 rotational transitions were

(47) Oka, T.; Morino, Y. *J. Mol. Spectrosc.* **1961**, *6*, 472-481.

(48) Oka, T.; Morino, Y. *J. Mol. Spectrosc.* **1963**, *11*, 349-367.

(49) Clouthier, D. J.; Ramsay, D. A. *Annu. Rev. Phys. Chem.* **1983**, *34*, 31-58.

(50) Morino, I.; Yamada, K.; Klein, H.; Belov, S. P.; Winniewisser, G.; Bocquet, R.; Wlodarczyk, G.; Lodyga, W.; Kreglewski, M. *J. Mol. Struct.* **2000**, *517*, 367-373.

(51) Cazzoli, G.; Lister, D. G.; Favero, P. G. *J. Mol. Spectrosc.* **1972**, *42*, 286-295.

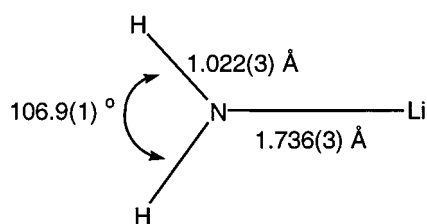
(52) Gordy, W.; Cook, R. L. *Microwave Molecular Spectra*; Wiley: New York, 1984; p 691.

(53) Wharton, L.; Gold, P.; Klemperer, W. *J. Chem. Phys.* **1962**, *37*, 2149-2150.

**Table 3.** Structural Parameters for  $\text{LiNH}_2$  and Related Species ( $\text{LiNH}_2$ )<sub>n</sub> (M = Li),  $\text{NaNH}_2$  (M = Na),  $\text{NH}_2^-$ , and  $\text{NH}_2$ 

species	source	$r_{\text{M-N}}(\text{\AA})$	$r_{\text{N-H}}(\text{\AA})$	$\theta_{\text{H-N-H}}(\text{deg})$	ref
$\text{LiNH}_2$	mm-wave ( $r_0$ structure)	1.736(3)	1.022(3)	106.9(1)	this work
	ab initio (STO-3G)	1.635	1.026	102.3	56
	ab initio	1.782	1.01 <sup>a</sup>	110	55
	ab initio (3-21G basis set)	1.714	1.013	106.5	24
	ab initio (3-21+G basis set)	1.759	1.013	107.0	24
	ab initio (3-21G basis set)	1.715	1.013	106.48	61
	ab initio (4-31+G basis set)	1.754	1.005	107.58	61
	ab initio (6-31G basis set)	1.74	1.01	108	24
	ab initio (6-31G* basis set)	1.750	1.005	105.25	61
	ab initio (6-31G)	1.740	1.016	106.5	57
	ab initio (6-31G**)	1.739	1.009	104.4	57
	ab initio (6-31G*)	1.750	1.005	105.2	58
	ab initio (SBK*)	1.786	1.019	103.8	58
	ab initio (TZV*)	1.728	1.002	105.2	58
	DMOL-min	1.697	1.134	100.8	59
	DMOL-DNP	1.731	1.033	104.0	59
	ab initio (MP2/6-311G*)	1.739	1.014	105.6	59
	ab initio (MP2/6-311+G*)	1.760	1.016	105.2	59
	ab initio (MIDI-4*)	1.767	1.011	103.9	62
	ab initio (MP2/6-31++G**)	1.754	nd	nd	63
B3LYP/6-31++G**	1.737	1.017	104.36	60	
B3LYP/6-31++G**(3df,2p)	1.732	1.015	104.27	60	
( $\text{LiNH}_2$ ) <sub>2</sub>	ab initio <sup>b</sup>	1.869–1.943 <sup>b</sup>	1.007–1.016 <sup>b</sup>	101.7–106 <sup>b</sup>	24
( $\text{LiNH}_2$ ) <sub>3</sub>	ab initio <sup>b</sup>	1.850–1.95 <sup>b</sup>	1.017–1.019 <sup>b</sup>	102.3–110 <sup>b</sup>	24
( $\text{LiNH}_2$ ) <sub>4</sub>	ab initio <sup>b</sup>	1.906–2.027 <sup>b</sup>	1.019	104.4–105.9 <sup>b</sup>	25
( $\text{LiNH}_2$ ) <sub>6</sub>	ab initio <sup>b</sup>	1.844–2.055 <sup>b</sup>	1.018–1.032 <sup>b</sup>	100.6–105.7 <sup>b</sup>	26
( $\text{LiNH}_2$ ) <sub>8</sub> <sup>c</sup>	X-ray crystallography	2.059(3), 2.064(9), 2.212(9), 2.213(3)	0.70(10), 0.76(12)	nd	11
$\text{NaNH}_2$	mm-wave ( $r_0$ structure)	2.091(3)	1.008(3)	106.6(1)	46 and this work
	ab initio (6-31G*)	2.080	1.007	104.4	58
	ab initio (SBK*)	2.150	1.022	103.0	58
	ab initio (TZV*)	2.096	1.005	104.6	58
	B3LYP/6-31++G**	2.097	1.017	104.93	60
	B3LYP/6-31++G**(3df,2p)	2.082	1.014	104.79	60
( $\text{NaNH}_2$ ) <sub>16</sub> <sup>d</sup>	X-ray crystallography	2.38–2.50	nd	nd	9
$\text{NH}_2^-$	infrared spectroscopy		1.041	102.1	64
$\text{NH}_2$	laser magnetic resonance		1.025	103.1	65

<sup>a</sup> Assumed value. <sup>b</sup> Values depend on geometry assumed and particular basis set employed. <sup>c</sup> 8 molecules in the unit cell. <sup>d</sup> 16 molecules in the unit cell.

**Scheme 2**

measured, including  $K_a$  components up to  $K_a = 5$ , over the frequency range 110–540 GHz. For  $\text{LiND}_2$ , 60 rotational transitions were recorded for components as high as  $K_a = 6$ . The final constants determined for these species are presented in Table 1, including the root mean square of the data fits, which indicate an analysis of high precision.

The structure was calculated using a least-squares routine, which determines the bond distances and angles using the moment of inertia equations (e.g. ref 52). The moments of inertia are obtained directly from the measured rotational constants. However, there are three unknowns involved in the structure for  $\text{LiNH}_2$  and only two such equations, because the molecule is planar. Therefore, two sets of equations were used, one using the moments for  $\text{LiNH}_2$  and the other those of  $\text{LiND}_2$ , assuming that the bond lengths do not change with isotopic substitution. The least-squares routine obtained the best fit to the structure using those four equations. Hence, the  $r_0$  structure portrayed in Scheme 2 was obtained.

**Comparison of Geometrical Parameters with Other Data.**

First we will discuss the overall geometry of the  $\text{M-NH}_2$  unit,

then we will focus on specific bond length and angle data. Although several groups have theoretically predicted a planar structure for  $\text{LiNH}_2$  (Table 3), the gas-phase data presented here are the first experimental confirmation of this fact and the most direct comparison between experiment and theory. In the previously reported structures of solid lithium and sodium amide, most attention was paid to the arrangement of amide anions and alkali metal cations in the crystal. As the data in Table 3 indicate, the lithium and sodium congeners contain 8 and 16 molecules, respectively, in their unit cells. Significantly, whereas our data show that both monomeric  $\text{LiNH}_2$  and  $\text{NaNH}_2$  are planar, the crystal packing of solid samples of these species made it impossible to say whether individual  $\text{MNH}_2$  units were planar or tetrahedral.<sup>9,11</sup> Only in the structure of solid  $\text{LiNH}_2$  was it possible to identify the positions of the H atoms.<sup>11</sup> However, in the best reported crystal structure of  $\text{LiNH}_2$  relatively large standard deviations in H-atom positions precludes meaningful comparison of N–H bond length and H–N–H angle with our gas-phase data. In addition, the fundamental difficulty with crystal data is that the orientation of each of the eight amide anions in the unit cell of  $\text{LiNH}_2$  clearly varies, precluding any conclusion about the geometry of a hypothetical  $\text{LiNH}_2$  monomeric unit in the crystal. Only in later structures of monomeric, solvated  $\text{M-NR}_2$  or  $\text{M-NHR}$  (for examples, see Scheme 1) was it possible to see that the  $\text{M-NR}_2$  unit was planar, but in these samples the R groups are very large or contain groups capable of delocalizing negative charge, features expected to encourage planarity. The Li–N bond distance in  $\text{LiNH}_2$  is 0.16 Å shorter than that in **1** (Scheme

1), which to our knowledge is the lithium amide featuring the shortest Li–N bond to date. This difference underscores the combined effects of solvation and large nitrogen substituents in increasing the bond distance. The observed M–N distance in  $\text{NaNH}_2$ <sup>46</sup> is longer than that in  $\text{LiNH}_2$ , as expected. The H–N–H angle in  $\text{NaNH}_2$  is  $106.6^\circ$ , based on new data obtained by Sheridan and Ziurys for  $\text{NaNd}_2$  (see Supporting Information). Therefore, this angle is almost identical to that in  $\text{LiNH}_2$  [ $106.9(1)^\circ$ ], a result in complete agreement with the relatively constant H–C–H angle in  $\text{M–CH}_3$  (M = Li, Na, K).<sup>54</sup>

Approximately 20 calculated structures for  $\text{LiNH}_2$  monomer have been reported in the literature, yet our data provide the first direct experimental test. From Table 3 it appears that earlier lower level calculations<sup>55,56</sup> gave the poorest results, whereas higher level ab initio calculations with 6-31G or larger basis sets provide the best structures.<sup>24,57–60</sup> Of note is a recent

(54) Grotjahn, D. B.; Pesch, T. C.; Brewster, M. A.; Ziurys, L. M. *J. Am. Chem. Soc.* **2000**, *122*, 4735–4741.

(55) Hinchliffe, A.; Dobson, J. C. *Theor. Chim. Acta* **1975**, *39*, 17–24.

(56) Dill, J. D.; Schleyer, P. v. R.; Binkley, J. S.; Pople, J. A. *J. Am. Chem. Soc.* **1977**, *99*, 6159–6173.

(57) Armstrong, D. R.; Perkins, P. G.; Walker, G. T. *J. Mol. Struct. (THEOCHEM)* **1985**, *122*, 189–203.

(58) Burk, P.; Koppel, I. *Int. J. Quantum Chem.* **1994**, *51*, 313–318.

(59) Pratt, L. M.; Khan, I. M. *J. Comput. Chem.* **1995**, *16*, 1067–1080.

(60) Schleyer, P. v. R. Private communication.

(61) Würthwein, E.-U.; Sen, K. D.; Pople, J. A.; Schleyer, P. v. R. *Inorg. Chem.* **1983**, *22*, 496–503.

(62) Koizumi, T.; Morihashi, K.; Kikuchi, O. *Bull. Chem. Soc. Jpn.* **1996**, *69*, 305–309.

(63) Kremer, T.; Harder, S.; Junge, M.; Schleyer, P. v. R. *Organometallics* **1996**, *15*, 585–595.

comparison of these methods with DFT calculations, which can also give good geometries as shown by results with DMOL-DNP.<sup>59</sup>

## Conclusions

The simplest lithium amide,  $\text{LiNH}_2$ , serves as a model for larger amides used in synthesis and structural studies. Its structure has been predicted several times in the literature, without direct experimental evidence for comparison until now. Here, gas-phase synthesis led to formation of the unsolvated monomer  $\text{LiNH}_2$  and microwave spectroscopy allowed its precise structure to be determined. The data here verify prediction of its planarity, showing in addition that higher level ab initio and DFT calculations provide accurate structural information. The results show the usefulness of gas-phase data on low-coordinate organometallic complexes, which will be the subject of further reports.

**Acknowledgment.** This research was supported by National Science Foundation grant CHE 9531244 (to D.B.G. and L.M.Z.) and NASA grant NAG 5-3785 (to L.M.Z.).

**Supporting Information Available:** Observed transitions for  $\text{NaNd}_2$  (PDF). This material is available free of charge via the Internet at <http://pubs.acs.org>.

JA003422H

(64) Tack, L. M.; Rosenbaum, N. H.; Owrtsky, J. C.; Saykally, R. J. *J. Chem. Phys.* **1986**, *84*, 7056–7057.

(65) Davies, P. B.; Russell, D. K.; Thrush, B. A.; Radford, H. E. *Proc. R. Soc. London A* **1977**, *353*, 299–318.